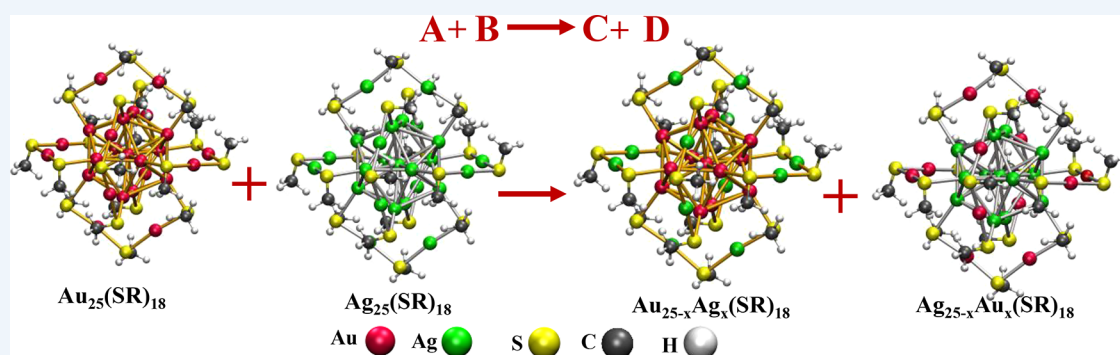


Interparticle Reactions: An Emerging Direction in Nanomaterials Chemistry

K. R. Krishnadas, Ananya Bakshi,[†] Atanu Ghosh, Ganapati Natarajan, Anirban Som, and Thalappil Pradeep*[‡]

Department of Chemistry, DST Unit of Nanoscience (DST UNS) and Thematic Unit of Excellence (TUE) Indian Institute of Technology Madras, Chennai 600 036, India



CONSPECTUS: Nanoparticles exhibit a rich variety in terms of structure, composition, and properties. However, reactions between them remain largely unexplored. In this *Account*, we discuss an emerging aspect of nanomaterials chemistry, namely, interparticle reactions in solution phase, similar to reactions between molecules, involving atomically precise noble metal clusters. A brief historical account of the developments, starting from the bare, gas phase clusters, which led to the synthesis of atomically precise monolayer protected clusters in solution, is presented first. Then a reaction between two thiolate-protected, atomically precise noble metal clusters, $[\text{Au}_{25}(\text{PET})_{18}]^{-}$ and $[\text{Ag}_{44}(\text{FTP})_{30}]^{4-}$ (PET = 2-phenylethanethiol, FTP = 4-fluorothiophenol), is presented wherein these clusters spontaneously exchange metal atoms, ligands, and metal–ligand fragments between them under ambient conditions. The number of exchanged species could be controlled by varying the initial compositions of the reactant clusters. Next, a reaction of $[\text{Au}_{25}(\text{PET})_{18}]^{-}$ with its structural analogue $[\text{Ag}_{25}(\text{DMBT})_{18}]^{-}$ (DMBT = 2,4-dimethylbenzenethiol) is presented, which shows that atom-exchange reactions happen with structures conserved. We detected a transient dianionic adduct, $[\text{Ag}_{25}\text{Au}_{25}(\text{DMBT})_{18}(\text{PET})_{18}]^{2-}$, formed between the two clusters indicating that this adduct could be a possible intermediate of the reaction. A reaction involving a dithiolate-protected cluster, $[\text{Ag}_{29}(\text{BDT})_{12}]^{3-}$ (BDT = 1,3-benzenedithiol), is also presented wherein metal atom exchange alone occurs, but with no ligand and fragment exchanges. These examples demonstrate that the nature of the metal–thiolate interface, that is, its bonding network and dynamics, play crucial roles in dictating the type of exchange processes and overall rates. We also discuss a recently proposed structural model of these clusters, namely, the Borromean ring model, to understand the dynamics of the metal–ligand interfaces and to address the site specificity and selectivity in these reactions.

In the subsequent sections, reactions involving atomically precise noble metal clusters and one- and two-dimensional nanosystems are presented. We show that highly protected, stable clusters such as $[\text{Au}_{25}(\text{PET})_{18}]^{-}$ undergo chemical transformation on graphenic surfaces to form a bigger cluster, $\text{Au}_{135}(\text{PET})_{57}$. Finally, we present the transformation of tellurium nanowires (Te NWs) to Ag–Te–Ag dumbbell nanostructures through a reaction with an atomically precise silver cluster, $\text{Ag}_{32}(\text{SG})_{19}$ (SG = glutathione thiolate).

The starting materials and the products were characterized using high resolution electrospray ionization mass spectrometry, matrix assisted laser desorption ionization mass spectrometry, UV/vis absorption, luminescence spectroscopies, etc. We have analyzed principally mass spectrometric data to understand these reactions.

In summary, we present the emergence of a new branch of chemistry involving the reactions of atomically precise cluster systems, which are prototypical nanoparticles. We demonstrate that such interparticle chemistry is not limited to metal clusters; it occurs across zero-, one-, and two-dimensional nanosystems leading to specific transformations. We conclude this *Account* with a discussion of the limitations in understanding of these reactions and future directions in this area of nanomaterials chemistry.

■ INTRODUCTION

Reactions between molecules have been explored ever since the beginning of chemistry. Atomic level understanding of chemical

Received: May 4, 2017

Published: July 20, 2017



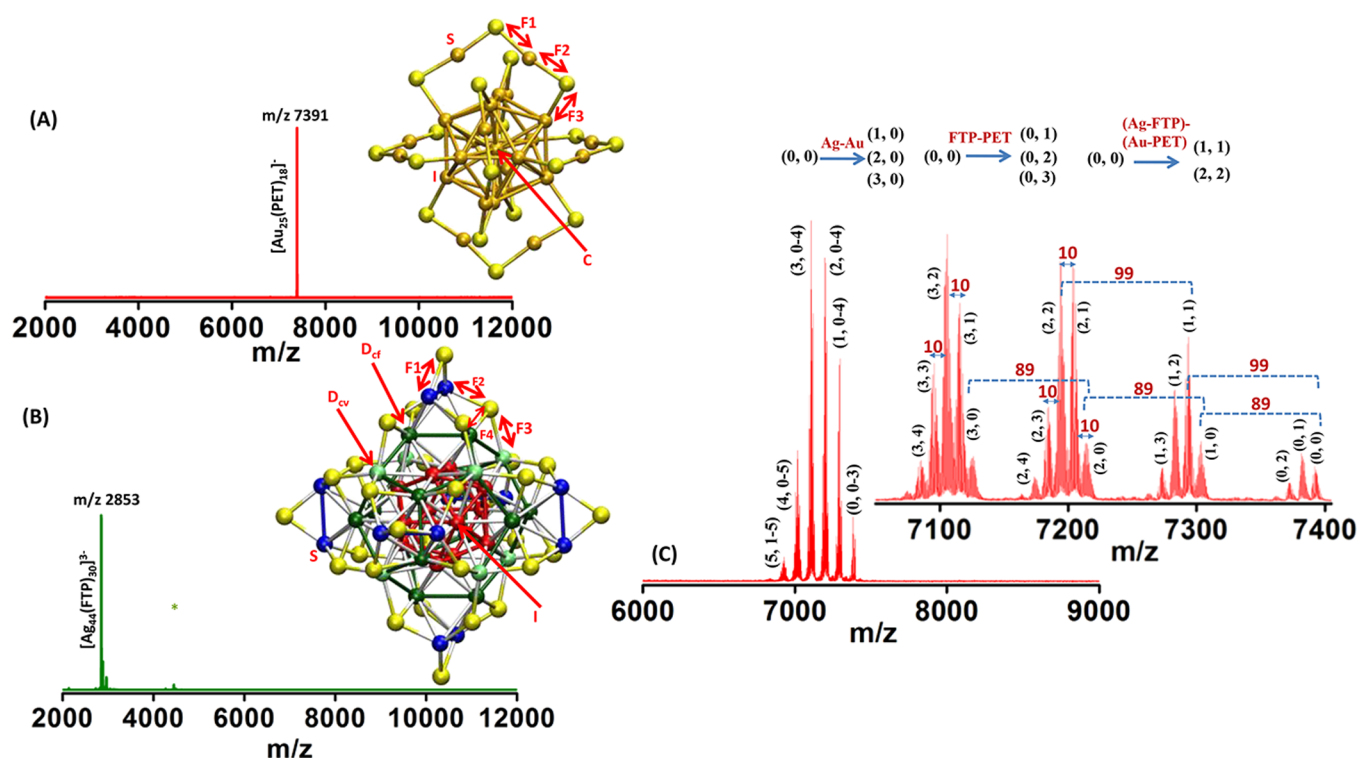


Figure 1. ESI mass spectra of (A) $\text{Au}_{25}(\text{PET})_{18}$, (B) $\text{Ag}_{44}(\text{FTP})_{30}$, and (C) a mixture of the two at $\text{Au}_{25}(\text{PET})_{18}:\text{Ag}_{44}(\text{FTP})_{30}$ molar ratio of 14.0:1.0 showing the formation of $\text{Au}_{25-x}\text{Ag}_x(\text{PET})_{18-y}(\text{FTP})_y$. Peaks at m/z 7391 in panel A and m/z 2853 in panel B are due to $[\text{Au}_{25}(\text{PET})_{18}]^-$ and $[\text{Ag}_{44}(\text{FTP})_{30}]^{3-}$, respectively. The numbers (x, y) of peak labels in (C) are according to the formula, $\text{Au}_{25-x}\text{Ag}_x(\text{PET})_{18-y}(\text{FTP})_y$. The peak labeled with * in panel B is due to $[\text{Ag}_{46}(\text{FTP})_{31}]^{2-}$ (see ref 34). Schematic structures of the clusters in insets show symmetry-unique Ag and Au atoms and Ag–S and Au–S bonds. Color codes: Au (orange), S (light yellow), Ag at the vertices of the cube of the Ag_{20} dodecahedron (D_{3h} ; light green), Ag at the faces of this cube (D_{3h} ; dark green). Ag in the mounts (S; blue). F1–F4 are distinct M–S (M = Ag or Au) bonds in $\text{Au}_{25}(\text{SR})_{18}$ and $\text{Ag}_{44}(\text{SR})_{30}$. The peaks (0, 0–3)–(3, 0–4) in panel C are expanded in the inset, assigning them to various exchange processes. Adapted with permission from ref 34. Copyright 2016 American Chemical Society.

transformations in terms of breaking and making of bonds is a central theme of chemical science. Just as molecules do, nanoparticles also exhibit a rich variety in terms of structure, composition, and properties. This diversity unveils a rarely explored landscape of chemical reactions occurring between nanoparticles. Atomic level understanding of such reactions require precise molecular entities, as model nanosystems, and precise molecular tools. Interparticle reactions have to be understood in the framework of established principles of chemistry. This Account present the beginnings of such an area, using ligand protected, atomically precise noble metal clusters, which are one of the most thoroughly explored classes of nanomaterials.

Atomically precise noble metal clusters are often studied in the form of unprotected entities^{1,2} either in the gaseous phase³ or supported on surfaces.⁴ Reactions of such clusters have been explored mostly with small molecules.^{1,3} However, understanding solution phase chemistry of clusters is essential for convenient investigations of their reactions and to explore their practical applications. One of the ways of making atomically precise noble metal clusters in solution is to use molecular ligands for controlled growth. Such clusters, protected with phosphines, were known from late 1970s.⁵ The introduction of alkyl or aryl thiolates (denoted as –SR) marked a resurgence in this field, about a decade ago. Pioneering efforts by Brust and Schiffrin⁶ and mass spectrometric measurements by Whetten et al. and Tsukuda et al. showed that highly monodisperse, molecule-like, thiolate-protected noble metal particles can be

synthesized in solution.^{7,8} Kornberg et al. resolved the first crystal structure of a thiolate-protected, atomically precise gold cluster,⁹ $\text{Au}_{102}(\text{SR})_{44}$, and later, Murray's and Jin's groups reported the structures^{10,11} of $[\text{Au}_{25}(\text{SR})_{18}]^-$. Zheng et al. reported the first crystal structure¹² of a thiolate-protected atomically precise silver cluster, $\text{Ag}_{14}(\text{SC}_6\text{H}_3\text{F}_2)_{12}(\text{PPh}_3)_8$. Later on, structures of $\text{Ag}_{16}(\text{DPPE})_4(\text{SR})_{14}$ and $[\text{Ag}_{32}(\text{DPPE})_5(\text{SR})_{24}]^{2-}$ (DPPE is 1,2-bis(diphenylphosphino)ethane) and $[\text{Ag}_{44}(\text{SR})_{30}]^{4-}$ were reported.^{13,14} Such clusters exhibit a number of unique properties as described elsewhere.^{15,16}

The availability of ligand protected clusters with accurately known structures opened up the possibility to explore their chemistry in greater detail. Substitution of metal atoms^{17,18} and the ligands,^{19–22} two fundamental structural components of ligand-protected metal clusters, are the major classes of their reactions. Metal ions and metal thiolates interact with the core and the ligands of these clusters, leading to (i) their decomposition or alloying²³ and (ii) changes in their optical absorption and emission features, which were utilized for the detection of trace levels of metal ions.^{24–26} Structural²⁷ and stereo²⁸ isomerisms of these clusters are emerging aspects. Electrochemical studies revealed distinct charge states of these clusters and their utility as redox catalysts²⁹ and biosensors.³⁰ Reactions of silver clusters with halocarbons were utilized for the degradation and removal of pesticides from water.³¹ Apart from these reactions, clusters are expected to react with themselves. For example, Murray et al. and Niihori et al. observed the exchange of metal atoms and the ligands between metal

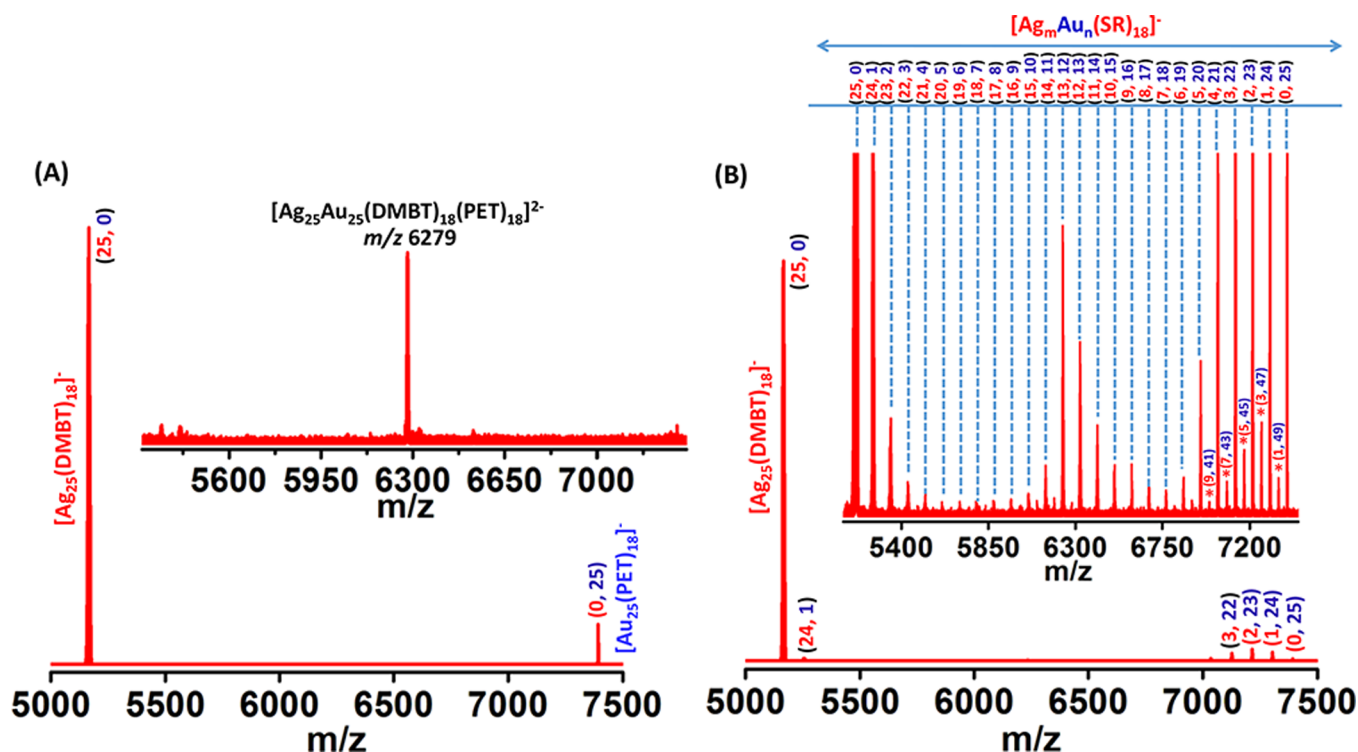


Figure 2. ESI mass spectra of a mixture of $\text{Ag}_{25}(\text{DMBT})_{18}$ and $\text{Au}_{25}(\text{PET})_{18}$ at a $\text{Ag}_{25}(\text{DMBT})_{18}:\text{Au}_{25}(\text{PET})_{18}$ molar ratio of 0.3:1.0 measured within 2 min after mixing (A) and after 5 min (B). The peak labels in panels A and B shown as numbers in red (m) and blue (n) in parentheses give the numbers of Ag and Au atoms, respectively, in the alloy clusters of the formula, $[\text{Ag}_m\text{Au}_n(\text{SR})_{18}]^1$. Numbers in the parentheses of the labels of the peaks marked with * in panel B correspond to the general formula $[\text{Ag}_m\text{Au}_n(\text{SR})_{36}]^{2-}$ ($m+n=50$), corresponding to the dianionic adducts. Adapted with permission from ref 38. Copyright 2016 Nature Publishing Group.

nanoparticles³² and clusters,³³ however, details of such processes remained unknown.

In this Account, we demonstrate interparticle reactions in solution phase using thiolate protected, atomically precise noble metal clusters, such as $[\text{Au}_{25}(\text{PET})_{18}]^-$, $[\text{Ag}_{25}(\text{DMBT})_{18}]^-$, $[\text{Ag}_{44}(\text{FTP})_{30}]^{4-}$, and $[\text{Ag}_{29}(\text{BDT})_{12}]^{3-}$. PET (2-phenylethanthiol), DMBT (2,4-dimethylbenzenethiol), FTP (4-fluorothiophenol), and BDT (1,3-benzenedithiol) are the ligands protecting the Au_{25} , Ag_{25} , Ag_{44} , and Ag_{29} cores, respectively. Typically these clusters are charged, as shown above; however, we denote them as $\text{Au}_{25}(\text{PET})_{18}$, $\text{Ag}_{44}(\text{FTP})_{30}$, etc., in the subsequent discussion for convenience. We begin this Account with a reaction between $[\text{Au}_{25}(\text{PET})_{18}]^-$ and $[\text{Ag}_{44}(\text{FTP})_{30}]^{4-}$ wherein these clusters spontaneously exchange metal atoms, ligands, and metal–ligand fragments between them under ambient conditions. Then we show that such processes can be structure-conserving, using a reaction between two structurally analogous clusters, $[\text{Au}_{25}(\text{PET})_{18}]^-$ and $[\text{Ag}_{25}(\text{DMBT})_{18}]^-$. A reaction involving a dithiolate-protected cluster, $[\text{Ag}_{29}(\text{BDT})_{12}]^{3-}$, is also demonstrated, which suggests that the nature of the metal–thiolate interface dictates the type of exchange processes and overall rates. A new structural model of these clusters, namely, the Borromean ring model, which we believe important to understand their exchange chemistry with site specificity, is also presented. Finally, we discuss reactions of noble metal clusters, which are zero-dimensional, with two- and one-dimensional nanostructures such as graphenic surfaces and tellurium nanowires (Te NWs), respectively, which show that chemical reactions indeed occur between nanosystems of any dimensionality. We conclude with a brief discussion of the limitations of such reactions and future directions.

REACTION BETWEEN $\text{Au}_{25}(\text{PET})_{18}$ AND $\text{Ag}_{44}(\text{FTP})_{30}$

The molecular formulae and structures (see insets of Figure 1) of $\text{Au}_{25}(\text{PET})_{18}$ and $\text{Ag}_{44}(\text{FTP})_{30}$ were determined previously using mass spectrometry and single crystal X-ray crystallography, respectively.^{10,11,14} Electrospray ionization (ESI) mass spectra (MS) of $\text{Au}_{25}(\text{PET})_{18}$ (Figure 1A) and $\text{Ag}_{44}(\text{FTP})_{30}$ (Figure 1B) show their expected features. In spite of their high stability due to their (i) compact cores, Au_{13} and Ag_{32} , being protected by $\text{Au}_2(\text{PET})_3$ staple motifs and $\text{Ag}_2(\text{FTP})_5$ mounts, respectively, and (ii) closed valence shell electronic configurations, we demonstrated that these clusters spontaneously react with each other in solution, exchanging metal atoms, ligands, and metal–ligand fragments between them.^{34,35}

Figure 1C shows the mass spectrum of a mixture of these two clusters wherein a series of peaks are observed. The mass difference between the peaks (1, 0), (2, 0), (3, 0), etc., is m/z 89 and hence these peaks are due to the Ag–Au exchanges between $\text{Au}_{25}(\text{PET})_{18}$ and $\text{Ag}_{44}(\text{FTP})_{30}$. The mass difference between the peaks (0, 1), (0, 2), (0, 3), etc., is m/z 10, and these peaks are due to the FTP–PET exchanges between the clusters. Apart from these, a set of peaks (1, 1), (2, 2), (3, 3), etc., are also observed, having mass difference of m/z 99, which are assigned to the exchanges of Ag–FTP and Au–PET fragments. Hence, the peaks in Figure 1C are assigned to the alloy clusters of the formula, $\text{Au}_{25-x}\text{Ag}_x(\text{PET})_{18-y}(\text{FTP})_y$, formed by exchanging metal atoms, ligands, and metal–ligand fragments. The maximum number of Ag incorporations observed so far in the case of all thiolate-protected $\text{Au}_{25}(\text{SR})_{18}$ clusters³⁶ is 11. However, we observed Ag substitution of up to 16–20 atoms into $\text{Au}_{25}(\text{SR})_{18}$ at higher concentrations of $\text{Ag}_{44}(\text{FTP})_{30}$.³⁴ Such a large number of heteroatom incorporation is unusual in cluster

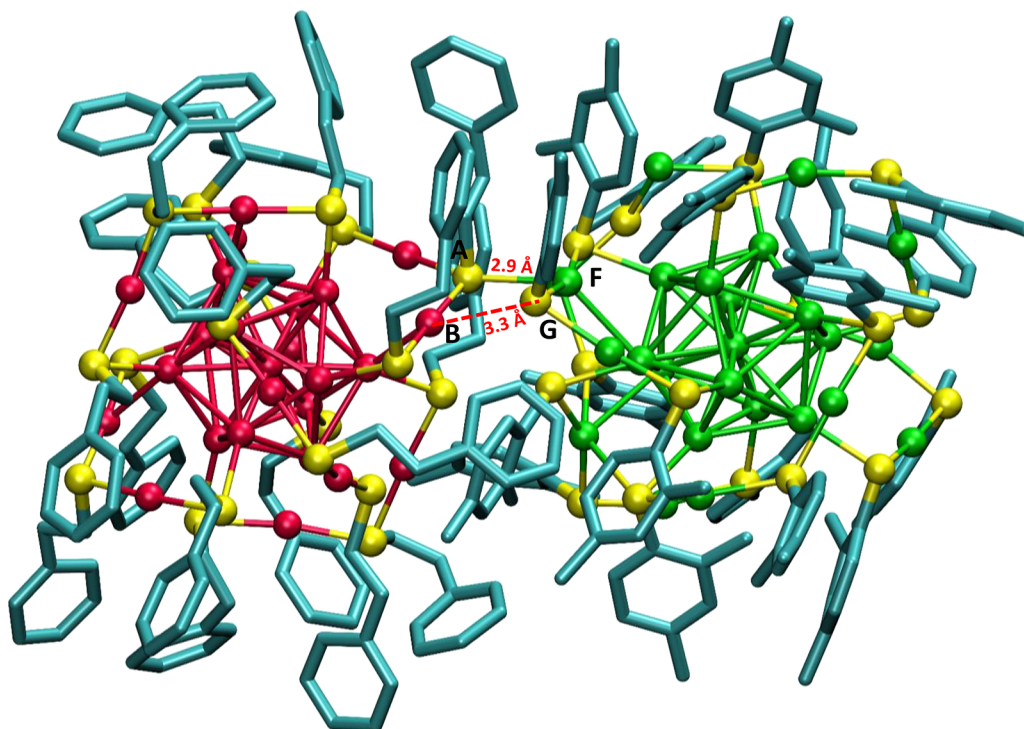


Figure 3. DFT-optimized geometry of $[\text{Ag}_{25}\text{Au}_{25}(\text{DMBT})_{18}(\text{PET})_{18}]^{2-}$ (with $\text{Ag}_{25}(\text{DMBT})_{18}$ on the right and $\text{Au}_{25}(\text{PET})_{18}$ on the left) formed in the reaction between $[\text{Ag}_{25}(\text{DMBT})_{18}]^{-}$ and $[\text{Au}_{25}(\text{PET})_{18}]^{-}$. The hydrogen atoms are omitted from the ligands for clarity. Color codes: Au (red), Ag (green), S (yellow), C (blue). Reproduced with permission from ref 38. Copyright 2016 Nature Publishing Group.

alloying, typically performed by using metal salts during synthesis. Note that the overall charge state and the total number of metal atoms and the ligands are preserved in the alloy clusters formed in this reaction. Ag atoms of $\text{Ag}_{44}(\text{FTP})_{30}$ get substituted with Au forming $\text{Au}_x\text{Ag}_{44-x}(\text{SR})_{30}$, whose formation correlates with the geometric and electronic shell structures of the reactants.³⁵

A number of questions, such as (i) how the two clusters approach each other overcoming the electrostatic repulsion resulting from the negative charges of the individual clusters and steric hindrance due to the ligands, (ii) whether intact clusters are involved in the reaction or any metal–thiolate fragments derived from one of the clusters is reacting with the other cluster, and (iii) whether there is any intermediate or adduct between the clusters formed during the reaction, remain unanswered. In the next section, we present a reaction that provides answers to some of these questions.

■ STRUCTURE-CONSERVING TRANSFORMATIONS

$\text{Au}_{25}(\text{PET})_{18}$ and $\text{Ag}_{25}(\text{DMBT})_{18}$ possess identical structural frameworks, that is, an inner M_{13} ($\text{M} = \text{Ag}/\text{Au}$) icosahedral core and six outer $\text{M}_2(\text{SR})_3$ staples.^{10,11,37} Unlike the previous example, the masses of the ligands, PET and DMBT, are equal, and hence the exchange of ligands (DMBT–PET exchange) and fragments ((Ag–DMBT)–(Au–PET) exchange), could not be detected; only the Ag–Au exchanges were detected.³⁸ The mass spectrum collected within 2 min after mixing the two clusters at a $\text{Ag}_{25}(\text{DMBT})_{18}:\text{Au}_{25}(\text{PET})_{18}$ molar of 0.3:1.0 is presented in Figure 2A wherein features of the parent clusters, along with a feature at m/z 6279 (see inset), which is due to a dianionic adduct, $[\text{Ag}_{25}\text{Au}_{25}(\text{DMBT})_{18}(\text{PET})_{18}]^{2-}$, formed between the clusters, are present. The mass spectrum of the same reaction mixture measured after 5 min (Figure 2B) shows that this adduct

vanished almost completely and a series of peaks separated by m/z 89 were observed (see inset of Figure 2B). Mass separation of 89 Da indicates the occurrence of Ag–Au exchange between $\text{Ag}_{25}(\text{DMBT})_{18}$ and $\text{Au}_{25}(\text{PET})_{18}$ resulting in the formation of entire range of alloy clusters, $[\text{Ag}_m\text{Au}_n(\text{SR})_{18}]$ ($n = 1\text{--}24$; $m + n = 25$), that is, $\text{Ag}_{24}\text{Au}_1(\text{SR})_{18}$ to $\text{Ag}_1\text{Au}_{24}(\text{SR})_{18}$, within this time scale. Since the DMBT–PET exchange is not detected for these alloys, the exact numbers of DMBT and PET ligands present in them are not known, and hence we use $-\text{SR}$ instead of both DMBT and PET separately in the general formula. The total number of metal atoms (25) and that of ligands (18) is preserved in the alloy clusters, as in the previous example.

The detection of $[\text{Ag}_{25}\text{Au}_{25}(\text{DMBT})_{18}(\text{PET})_{18}]^{2-}$ indicates that the two intact clusters themselves could participate in these “bimolecular” reactions, and this adduct could be a possible intermediate prior to the formation of alloys. A structure of the adduct, optimized using density functional theory (DFT) calculations, is shown in Figure 3, wherein a Ag–S bond between the staples of the clusters is observed. Bürgi et al. showed that no exchange occurs when the solutions of $\text{Ag}_x\text{Au}_{38-x}(\text{SR})_{24}$ and $\text{Au}_{38}(\text{SR})_{24}$ clusters³⁹ were separated by a dialysis membrane, which is impermeable to the clusters. The reactant clusters involved in our experiments were washed thoroughly using suitable solvents to remove free ligands and metal–ligand complexes. Therefore, we think that intact clusters are the actual species involved in the reactions, not free ligands or metal–thiolate fragments. UV/vis absorption and emission spectra of reaction mixtures are significantly different from that of the reactant clusters,^{34,38} which confirm that the reactions observed occur in bulk solution phase, not in evaporating droplets during electrospray ionization or in the gas phase.

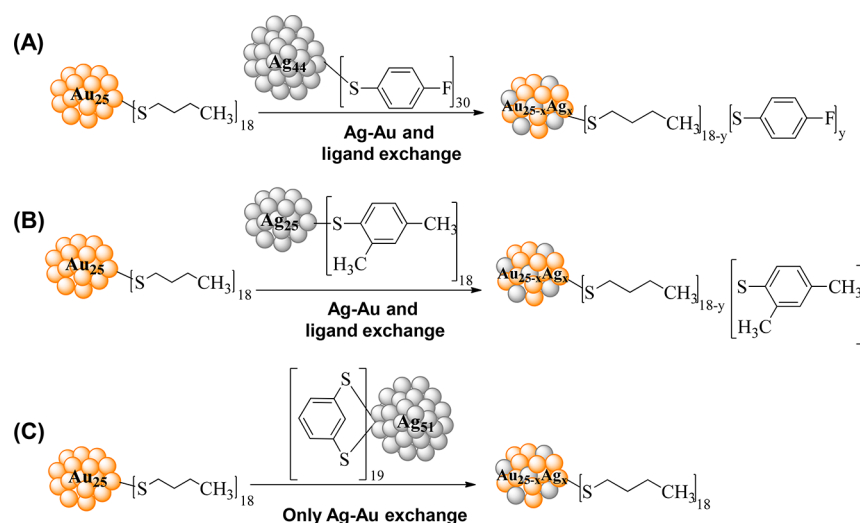


Figure 4. Schematic of the reactions between $\text{Au}_{25}(\text{BuS})_{18}$ with (A) $\text{Ag}_{44}(\text{FTP})_{30}$ (B) $\text{Ag}_{25}(\text{DMBT})_{18}$, and (C) $\text{Ag}_{51}(\text{BDT})_{19}$. Adapted with permission from ref 43. Copyright 2017 Royal Society Publishing Group.

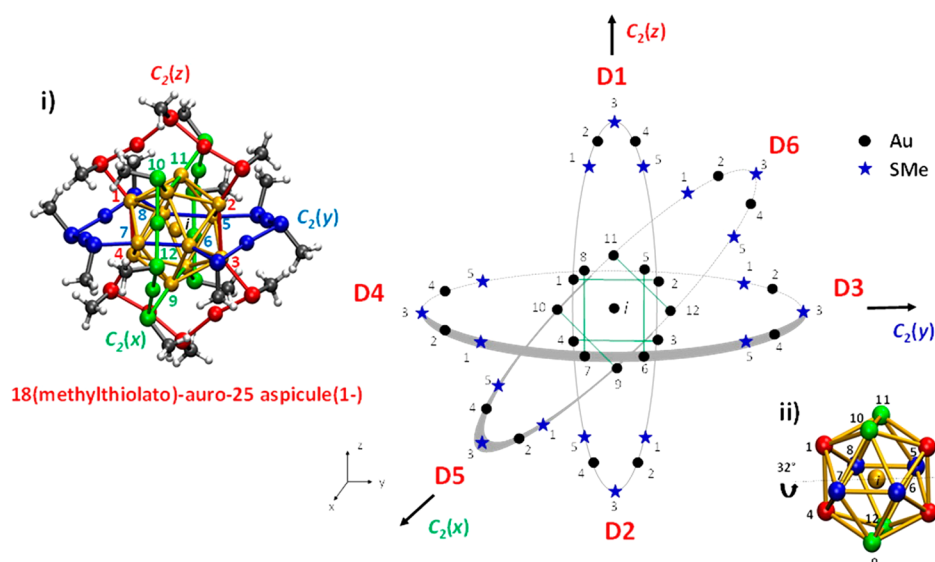


Figure 5. Borromean rings diagram of $\text{Au}_{25}(\text{SMe})_{18}$. The rings formed by pairs of coplanar staples are shown as ellipses. Gold atoms are shown by black dots, and dark blue stars represent the $-\text{SMe}$ ligands whose positions are taken to be identical to their sulfur atom. The core Au atoms are numbered from 1 to 12, and the staple atoms are numbered clockwise from end of the staple, from 1 to 5. The lines that join the core Au atoms on opposite ends of the same staple are shown by green lines. The three perpendicular C₂ axes are marked with the associated Cartesian axis direction in brackets. The staple directions are labeled by the six staple locants, D1 to D6, marked in red. Inset i shows a 3D visualization of the ring structure of the core and staples of $\text{Au}_{25}(\text{SR})_{18}$ aspicule, with each (Au_8S_6) -ring consisting of two coplanar staples and the core atoms that are bonded to these staples. The three rings are colored red, blue, and green, and the numbers of the core atoms are marked. Inset ii shows a close-up of the numbering scheme of the core atoms marked on the edge-projection of the core icosahedron. The arrow indicates the angle of the anticlockwise rotation about the y-axis needed to bring the icosahedron into a face-projected view of the face defined by the atoms 6, 7, and 9. Reproduced with permission from ref 47. Copyright 2015 American Chemical Society.

EXPERIMENTS WITH DITHIOLATE-PROTECTED CLUSTERS

The reactions discussed above show that metal atom, ligand, and metal–ligand fragments were exchanged between the clusters. Ligand and fragment exchanges show that the nature of ligands or metal–ligand interfaces play a role in such reactions. The ligands involved in the above examples are monothiolates, which are highly dynamic on the surfaces of clusters.^{40,41} This implies that spontaneous exchanges between the clusters could be due to the mobility^{40,41} of these ligands. One of the ways to control intercluster exchanges is to decrease the mobility of the ligands at

the metal–ligand interface by using dithiolate ligands, which can bind to the cluster surface in a bidentate fashion. Clusters such as $\text{Ag}_{29}(\text{BDT})_{12}$ and $\text{Ag}_{51}(\text{BDT})_{19}$ protected with BDT were reported^{42,43} wherein BDT acts as a bidentate ligand. Surprisingly, reactions between $\text{Ag}_{29}(\text{BDT})_{12}$ (or $\text{Ag}_{51}(\text{BDT})_{19}$) and a monothiolate-protected cluster such as $\text{Au}_{25}(\text{BuS})_{18}$ showed that only Ag–Au exchanges occurred; no ligand and metal–ligand fragment exchanges were observed (see Figure 4C). These reactions were significantly slower compared to those involving only monothiolate-protected clusters.

In $\text{M}_{25}(\text{SR})_{18}$ ($\text{M} = \text{Ag}/\text{Au}$; $-\text{SR}$ = a monothiolate) clusters, the ligands are monodentate and they form $\text{M}_2(\text{SR})_3$ staples. A

single M–S bond has to be broken in order to break these staple motifs, exposing the M_{13} icosahedral core, facilitating exchange reactions. Crystal structure of $Ag_{29}(BDT)_{12}$ shows that the BDT acts as a bidentate ligand.⁴² Therefore, more than one Ag–S bonds have to be broken in order to break the Ag–S bonding network for facilitating further reactions. Such bidentate bonding ligands make the metal–thiolate interface more rigid compared to the monothiolate-protected clusters. Therefore, we think that the rigidity of the metal–thiolate framework in $Ag_{29}(BDT)_{12}$ could be the key factor behind the absence of ligand and fragment exchanges and slow kinetics.

■ A NEW STRUCTURAL MODEL TO UNDERSTAND CLUSTER REACTIVITY

To comprehend the reactions presented so far, clearly in terms of atomic events, a systematic way of structural representation is needed. Thiolate-protected noble metal clusters have traditionally been viewed as consisting of a distinct core of metal atoms protected by a precise number of oligomeric metal–ligand units. For example, $Au_{25}(SR)_{18}$ can be considered as an icosahedral Au_{13} core protected by six $Au_2(SR)_3$ staples. New structural models^{44–47} for these clusters have emerged in the recent past. Among these, we think that the Borromean ring model⁴⁷ or *aspicule* (combination of the Greek word “aspis” meaning *shield* with “molecule”) model, wherein these clusters are viewed as composed of interlocked rings of metal thiolates (see Figure 5), would be useful in understanding their reactions. According to this model, an $M_{25}(SR)_{18}$ ($M = Ag/Au$) is considered as made up of three interlocked $M_8(SR)_6$ rings surrounding a central metal atom, M , that is, $M_{25}(SR)_{18}$ can be represented as $M@[M_8(SR)_6]_3$. The 24 metal atoms and 18 sulfur atoms in $M_{25}(SR)_{18}$, which were previously considered as part of the two distinct structural units, that is, the M_{13} icosahedral core and the six $M_2(SR)_3$ staples, are now parts of the unified structural motif, that is, the $M_8(SR)_6$ rings. Geometrical stability of such clusters is attributed to the interlocking of the rings, rather than the existence of a distinct and compact core protected by staple motifs.

We think that one of the reasons behind the spontaneous exchange reactions is the dynamics of the $M_8(SR)_6$ rings. When two reacting clusters approach each other, a M–S bond in one of the $M_8(SR)_6$ rings can undergo cleavage, and the open ends of this ring can undergo reactions with the adjacent clusters.³⁸ As mentioned earlier, the reactions involving monothiolates are faster compared to those involving dithiolates. This is attributed to the increased rigidity of metal thiolate rings when dithiolates are present. Another notable feature in these reactions is that the number of metal atoms and the ligands are unaltered. Hence, the spontaneous reactivity and preservation of the number of metal atoms and the ligands could be due to the stability of the alloy clusters, arising from the retention of the $M_8(SR)_6$ ring structure.

An important concern about the Borromean ring model is whether it represents the true solution phase geometry and chemical behavior of these clusters. This implies that a distinct core and a shell exist only in the solid state alone. We think that these clusters exist in the form of metal–thiolate rings in solution. The dynamics of the rings could be one of the reasons for spontaneous intercluster exchange reactions, which is supported by the reactions involving $Ag_{29}(BDT)_{12}$ wherein the reaction was slower probably because of a more rigid metal–thiolate framework. Another hint about the existence of the ring structure in solutions comes from the analysis of the number of metal atoms exchanged between the clusters. Note that more

than 12 Ag atoms could be incorporated into $Au_{25}(SR)_{18}$. If the cluster existed as a distinct Au_{13} core and $Au_2(SR)_3$ staples, in solution, incorporation of more than 12 Ag atoms may not be feasible because the metal atom sites in the M_{13} core will not be easily accessible due to protection by the staples. The Borromean ring model implies that all of the metal atoms, except the central one, are in identical environments and hence equally accessible for substitution. This similar accessibility could be one of the reasons for the facile substitution of more than 12 metal atoms in $Au_{25}(SR)_{18}$.

The Borromean ring model enables precise labeling of the positions of metal atoms and the ligands in thiolate protected clusters,⁴⁷ which opens up challenges to achieve site-specific metal atom substitution. Remember that in all the examples mentioned above, a mixture of products are obtained always. We note that though there are a few examples of site-specific substitution of ligands,⁴⁸ such specificity in metal atom substitution has not yet been achieved, except in the case of $Ag_{24}Au_1(SR)_{18}$ (ref 49). Recently, Bhat et al. showed that $Au_{22}Ir_3(PET)_{18}$ can be synthesized⁵⁰ exclusively by the reaction between the clusters $Au_{25}(PET)_{18}$ and $Ir_9(PET)_6$.

■ CLUSTERS WITH OTHER NANOSYSTEMS: NEW DIRECTIONS IN INTERPARTICLE INTERACTIONS

Coalescence of Ligand Protected Clusters on Graphenic Surfaces

Clusters supported on surfaces have been used as heterogeneous catalysts. Interaction of bare metal clusters with graphenic surfaces have also been studied.⁵¹ Interaction of ligand-protected clusters on such surfaces are rarely investigated. Anchoring of the ligands onto surfaces leads to changes in the geometric and electronic structures of the clusters, which in turn induce reactivity. In this section, we discuss a dramatic transformation of $Au_{25}(SR)_{18}$ on graphenic surfaces⁵² leading to the formation of $Au_{135}(SR)_{57}$ at room temperature, without the assistance of any catalyst or other chemicals (see Figure 6). Entrapment of the

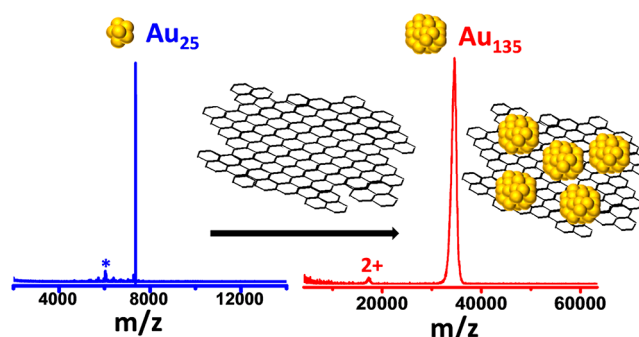


Figure 6. Schematic of the transformation of $Au_{25}(PET)_{18}$ to $Au_{135}(PET)_{57}$ on graphenic surfaces. Observation of the dicationic feature confirms the assignment. Adapted with permission from ref 52. Copyright 2014 American Chemical Society.

clusters in the inherent curvatures or local valleys of graphenic surfaces leading to the reduction in the surface curvature and associated energy gain of the overall system is considered to be the driving force behind such transformations. However, these results demonstrate that (i) highly protected clusters can undergo unexpected chemical transformations on surfaces and (ii) surfaces could be reactive substrates for such metal clusters, which could be a new methodology to synthesize clusters.

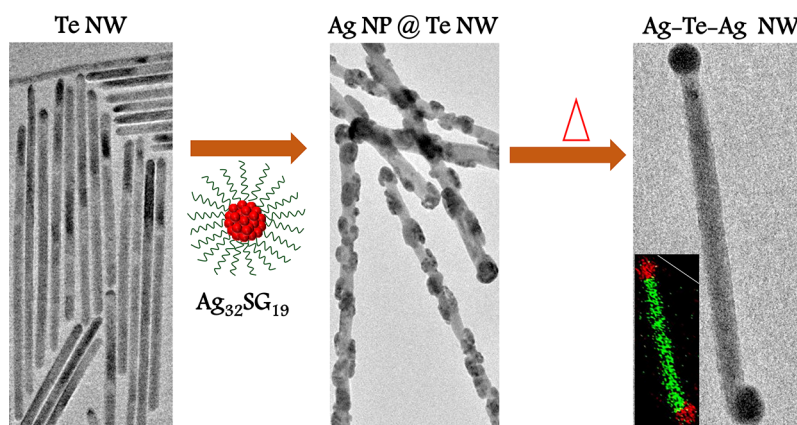


Figure 7. Schematic of the formation of Ag–Te–Ag NWs by the reaction between Te NWs and $\text{Ag}_{32}(\text{SG})_{19}$. Adapted with permission from ref 53. Copyright 2014 American Chemical Society.

Reaction of Clusters with One-Dimensional Nanostructures: New Ways for Hybrid Nanomaterials

Here we demonstrate that $\text{Ag}_{32}(\text{SG})_{19}$ (SG = glutathione thiolate)⁵³ reacts with Te NWs leading to the formation of silver nanoparticles (Ag NPs) on the surface of the NWs (see Figure 7). Upon heating, these Ag NP-decorated Te NWs were transformed to dumbbell shaped NWs wherein Ag NPs were present at the tips and the middle had only Te. This reaction demonstrates the utility of such chemistry toward creating novel nanostructures.

Reactions of Te NWs with Ag(I) ions and bigger plasmonic Ag NPs produced Ag_2Te NWs, and no dumbbell nanostructures were formed. These experiments show that atomically precise clusters exhibit distinct reactivity compared to larger nanoparticles or metal ions. This difference in reactivity is attributed to the fact that the rate of leaching of Ag atoms or ions are different for Ag NPs and atomically precise Ag clusters. Larger nanoparticles possess significantly higher numbers of Ag atoms with reduced coordination numbers compared to $\text{Ag}_{32}(\text{SG})_{19}$, which are highly protected by thiolate ligands. Though these clusters are protected by thiolate ligands, the protection is incomplete, and because of this, the clusters tend to coalesce at the surface of NWs, leading to Ag NPs.

■ LIMITATIONS AND FUTURE PERSPECTIVES

Currently, the intercluster exchange reactions were demonstrated only with noble metal clusters except a recent report involving copper clusters.⁵⁴ The structures of the product clusters are not known, however, and such information will provide further insights into these reactions. A mixture of alloy clusters were formed in these reactions since there are unique sites for the metal atoms, ligands, and metal–ligand fragments in the reactant clusters (see insets of Figure 1A,B); no specific product with a given composition was formed. Separation of these products into individual alloy clusters and their isomers has not yet been successful.

The driving force behind these reactions could be the lowering of the total energy due to metal or fragment substitution into symmetry unique positions in the reactant clusters.^{34,38} Difference in oxidation states of the metal atoms in the core and the staples may also contribute to the reactivity.

Details of the mechanistic aspects, such as (i) which of the clusters (Au_{25} or $\text{Ag}_{25}/\text{Au}_{25}$ or Ag_{44}) initiates the reaction, (ii) which of the bonds (metal–metal or metal–ligand) are broken first, (iii) what are the actual species (free metal atoms, ligands, or

metal–ligand fragments) being exchanged between the two clusters, are not known.

These reactions are to be looked at from the standard concepts of physical chemistry. Controlling the kinetics using catalysts or inhibitors or by changing temperature or pressure and quantitative determination of thermodynamic parameters such as reaction enthalpies, free energies, etc., are a few directions in this regard. Probing the reaction dynamics using molecular beam experiments and ab initio molecular dynamics is essential to understanding the mechanisms in detail.

Such reactions were demonstrated only with ligand-protected clusters. It is interesting to explore whether such reactions could occur between bare metal clusters, either in solution or in the gas phase. Extending these reactions to other types of nanosystems, such as quantum dots and inorganic and carbon clusters, can be a potential new route to create unprecedented types of hybrid nanomaterials. Two-dimensional nanosystems such as MoS_2 and graphene can also be suitable candidates for exploring these reactions. The presence of defects, surface atoms with low coordination numbers, etc., might induce reaction between these nanosystems. Stimuli, such as temperature, light, pressure, or mechanical strain,^{55,56} may also induce interparticle chemistry. Techniques such as high resolution mass spectrometry and ion mobility mass spectrometry are important in exploring the dynamics associated with such reactions. Computational methods are essential to understand the underlying events. We propose that chemical reactions between nanoparticles may be written down with structural details using the *aspicule* nomenclature. It is likely that in the foreseeable future, we will have enough understanding to describe nanoparticle chemistry with atomic precision, leading to products with compositional, structural, conformational, and even enantiomeric control.

■ AUTHOR INFORMATION

Corresponding Author

*E-mail: pradeep@iitm.ac.in.

ORCID 

Thalappil Pradeep: 0000-0003-3174-534X

Present Address

[†]A.B.: Postdoctoral fellow at Karlsruhe Institute of Technology, Germany.

Notes

The authors declare no competing financial interest.

Biographies

Krishnadas, after earning a Ph.D. in Chemistry from the Indian Institute of Technology Madras in 2016 under the guidance of Prof. T. Pradeep, is currently a postdoctoral researcher in the same group. He explores chemical reactions of atomically precise noble metal clusters.

Ananya Baksi, after earning a Ph.D. in Chemistry from the Indian Institute of Technology Madras in 2015 under the guidance of Prof. T. Pradeep, is currently a postdoctoral researcher at Karlsruhe Institute of Technology, Germany. Her research is focused on mass spectrometric investigations of different cluster systems.

Atanu Ghosh is a Ph.D. student at the Indian Institute of Technology Madras under the guidance of Prof. T. Pradeep. His research focuses on the synthesis, reactions, and applications of noble metal nanoclusters.

Ganapati Natarajan, after earning Ph.D. in Chemistry (2011) from the Department of Chemistry at the University of Cambridge, UK, is a postdoctoral researcher in Prof. Pradeep's research group. He is a computational materials scientist with interests in structure and properties of ligand-protected noble metal clusters and nanoparticles, ice, and amorphous materials.

Anirban Som, after earning a Ph.D. in Chemistry from the Indian Institute of Technology Madras in 2016 under the guidance of Prof. T. Pradeep, is currently a postdoctoral researcher in the same group. He explores the reactivity of tellurium nanowires, two-dimensional materials such as MoS₂, etc., using transmission electron microscopy.

T. Pradeep is an Institute Professor and Deepak Parekh Institute Chair Professor at the Indian Institute of Technology Madras. Prof. Pradeep's research interests are in molecular and nanoscale materials, and he develops instrumentation for such studies. He is involved in the development of affordable technologies for drinking water purification, and some of his technologies have been commercialized.

ACKNOWLEDGMENTS

K.R.K. and A.G. thank the UGC for their senior research fellowships. A.S. thanks the CSIR for his senior research fellowship. A.B. thanks IIT Madras for an Institute Post-Doctoral Fellowship. We thank the Department of Science and Technology for constantly supporting our research program.

REFERENCES

- (1) Johnston, R. L. *Atomic and Molecular Clusters*; Taylor and Francis: London, 2002.
- (2) Henglein, A. Physicochemical properties of small metal particles in solution: "microelectrode" reactions, chemisorption, composite metal particles, and the atom-to-metal transition. *J. Phys. Chem.* **1993**, *97*, 5457–5471.
- (3) Kappes, M. M. Experimental studies of gas-phase main-group metal clusters. *Chem. Rev.* **1988**, *88*, 369–389.
- (4) Gates, B. C. Supported Metal Clusters: Synthesis, Structure, and Catalysis. *Chem. Rev.* **1995**, *95*, 511–522.
- (5) Briant, C. E.; Theobald, B. R. C.; White, J. W.; Bell, L. K.; Mingos, D. M. P.; Welch, A. J. Synthesis and X-ray structural characterization of the centred icosahedral gold cluster compound [Au₁₃(PMe₂Ph)₁₀Cl₂](PF₆)₃; the realization of a theoretical prediction. *J. Chem. Soc., Chem. Commun.* **1981**, 201–202.
- (6) Brust, M.; Walker, M.; Bethell, D.; Schiffrin, D. J.; Whyman, R. Synthesis of thiol-derivatised gold nanoparticles in a two-phase Liquid-Liquid system. *J. Chem. Soc., Chem. Commun.* **1994**, 0, 801–802.
- (7) Whetten, R. L.; Khoury, J. T.; Alvarez, M. M.; Murthy, S.; Vezmar, I.; Wang, Z. L.; Stephens, P. W.; Cleveland, C. L.; Luedtke, W. D.; Landman, U. Nanocrystal gold molecules. *Adv. Mater.* **1996**, *8*, 428–433.

- (8) Negishi, Y.; Takasugi, Y.; Sato, S.; Yao, H.; Kimura, K.; Tsukuda, T. Magic-numbered Au_n clusters protected by glutathione monolayers (n = 18, 21, 25, 28, 32, 39): Isolation and spectroscopic characterization. *J. Am. Chem. Soc.* **2004**, *126*, 6518–6519.
- (9) Jadzinsky, P. D.; Calero, G.; Ackerson, C. J.; Bushnell, D. A.; Kornberg, R. D. Structure of a thiol monolayer-protected gold nanoparticle at 1.1 Å resolution. *Science* **2007**, *318*, 430–433.
- (10) Heaven, M. W.; Dass, A.; White, P. S.; Holt, K. M.; Murray, R. W. Crystal structure of the gold nanoparticle [N(C₈H₁₇)₄]-[Au₂₅(SCH₂CH₂Ph)₁₈]. *J. Am. Chem. Soc.* **2008**, *130*, 3754–3755.
- (11) Zhu, M.; Aikens, C. M.; Hollander, F. J.; Schatz, G. C.; Jin, R. Correlating the crystal structure of a thiol-protected Au₂₅ cluster and optical properties. *J. Am. Chem. Soc.* **2008**, *130*, 5883–5885.
- (12) Yang, H.; Lei, J.; Wu, B.; Wang, Y.; Zhou, M.; Xia, A.; Zheng, L.; Zheng, N. Crystal structure of a luminescent thiolated Ag nanocluster with an octahedral Ag₆⁴⁺ core. *Chem. Commun.* **2013**, 49, 300–302.
- (13) Yang, H.; Wang, Y.; Zheng, N. Stabilizing subnanometer Ag(0) nanoclusters by thiolate and diphosphine ligands and their crystal structures. *Nanoscale* **2013**, *5*, 2674–2677.
- (14) Desiredy, A.; Conn, B. E.; Guo, J.; Yoon, B.; Barnett, R. N.; Monahan, B. M.; Kirschbaum, K.; Griffith, W. P.; Whetten, R. L.; Landman, U.; Bigioni, T. P. Ultrastable silver nanoparticles. *Nature* **2013**, *501*, 399–402.
- (15) Mathew, A.; Pradeep, T. Noble metal clusters: Applications in energy, environment and biology. *Part. Part. Syst. Charact.* **2014**, *31*, 1017–1053.
- (16) Chakraborty, I.; Pradeep, T. Atomically precise clusters of noble metals: Emerging link between atoms and nanoparticles. *Chem. Rev.* **2017**, *117*, 8208–8271.
- (17) Wang, S.; Meng, X.; Das, A.; Li, T.; Song, Y.; Cao, T.; Zhu, X.; Jin, R. A 200-fold quantum yield boost in the photo-luminescence of silver-doped Ag₂₅ nanoclusters: The 13th silver atom matters. *Angew. Chem., Int. Ed.* **2014**, *53*, 2376–2380.
- (18) Negishi, Y.; Igarashi, K.; Munakata, K.; Ohgake, W.; Nobusada, K. Palladium doping of magic gold cluster Au₃₈(SC₂H₄Ph)₂₄: formation of Pd₂Au₃₆(SC₂H₄Ph)₂₄ with higher stability than Au₃₈(SC₂H₄Ph)₂₄. *Chem. Commun.* **2012**, 48, 660–662.
- (19) Guo, R.; Song, Y.; Wang, G.; Murray, R. W. Does core size matter in the kinetics of ligand exchanges of monolayer-protected Au clusters? *J. Am. Chem. Soc.* **2005**, *127*, 2752–2757.
- (20) Hassinen, J.; Pulkkinen, P.; Kalenius, E.; Pradeep, T.; Tenhu, H.; Hakkinen, H.; Ras, R. H. A. Mixed-monolayer-protected Au₂₅ clusters with bulky calix[4]arene functionalities. *J. Phys. Chem. Lett.* **2014**, *5*, 585–589.
- (21) Mathew, A.; Natarajan, G.; Lehtovaara, L.; Häkkinen, H.; Kumar, R. M.; Subramanian, V.; Jaleel, A.; Pradeep, T. Supramolecular functionalization and concomitant enhancement in properties of Au₂₅ clusters. *ACS Nano* **2014**, *8*, 139–152.
- (22) Muhammed, M. A. H.; Shaw, A. K.; Pal, S. K.; Pradeep, T. Quantum clusters of gold exhibiting FRET. *J. Phys. Chem. C* **2008**, *112*, 14324–14330.
- (23) Udayabhaskararao, T.; Sun, Y.; Goswami, N.; Pal, S. K.; Balasubramanian, K.; Pradeep, T. Ag₇Au₆: A 13-atom alloy quantum cluster. *Angew. Chem., Int. Ed.* **2012**, *51*, 2155–2159.
- (24) Habeeb Muhammed, M. A.; Pradeep, T. Reactivity of Au₂₅ clusters with Au³⁺. *Chem. Phys. Lett.* **2007**, *449*, 186–190.
- (25) Chakraborty, I.; Udayabhaskararao, T.; Pradeep, T. Luminescent sub-nanometer clusters for metal ion sensing: a new direction in nanosensors. *J. Hazard. Mater.* **2012**, *211–212*, 396–403.
- (26) Krishnadas, K. R.; Udayabhaskararao, T.; Choudhury, S.; Goswami, N.; Pal, S. K.; Pradeep, T. Luminescent AgAu alloy clusters derived from Ag nanoparticles - manifestations of tunable Au(I)-Cu(I) metallophilic interactions. *Eur. J. Inorg. Chem.* **2014**, *2014*, 908–916.
- (27) Tian, S.; Li, Y.-Z.; Li, M.-B.; Yuan, J.; Yang, J.; Wu, Z.; Jin, R. Structural isomerism in gold nanoparticles revealed by X-ray crystallography. *Nat. Commun.* **2015**, *6*, 8667.
- (28) Dolamic, I.; Knoppe, S.; Dass, A.; Bürgi, T. First enantioseparation and circular dichroism spectra of Au₃₈ clusters protected by achiral ligands. *Nat. Commun.* **2012**, *3*, 798.

- (29) Chong, H.; Li, P.; Wang, S.; Fu, F.; Xiang, J.; Zhu, M.; Li, Y. Au₂₅ clusters as electron-transfer catalysts induced the intramolecular cascade reaction of 2-nitrobenzonitrile. *Sci. Rep.* **2013**, *3*, 3214.
- (30) Kumar, S. S.; Kwak, K.; Lee, D. Amperometric sensing Based on glutathione protected Au₂₅ nanoparticles and their pH dependent electrocatalytic Activity. *Electroanalysis* **2011**, *23*, 2116–2124.
- (31) Bootharaju, M. S.; Pradeep, T. Understanding the degradation pathway of the pesticide, chlorpyrifos by noble metal nanoparticles. *Langmuir* **2012**, *28*, 2671–2679.
- (32) Song, Y.; Huang, T.; Murray, R. W. Heterophase ligand exchange and metal transfer between monolayer protected clusters. *J. Am. Chem. Soc.* **2003**, *125*, 11694–11701.
- (33) Niihori, Y.; Kurashige, W.; Matsuzaki, M.; Negishi, Y. Remarkable enhancement in ligand-exchange reactivity of thiolate-protected Au₂₅ nanoclusters by single Pd atom doping. *Nanoscale* **2013**, *5*, 508–512.
- (34) Krishnadas, K. R.; Ghosh, A.; Baksi, A.; Chakraborty, I.; Natarajan, G.; Pradeep, T. Intercluster reactions between Au₂₅(SR)₁₈ and Ag₄₄(SR)₃₀. *J. Am. Chem. Soc.* **2016**, *138*, 140–148.
- (35) Krishnadas, K. R.; Baksi, A.; Ghosh, A.; Natarajan, G.; Pradeep, T. Manifestation of geometric and electronic shell structures of metal clusters in intercluster reactions. *ACS Nano* **2017**, *11*, 6015–6023.
- (36) Negishi, Y.; Iwai, T.; Ide, M. Continuous modulation of electronic structure of stable thiolate-protected Au₂₅ cluster by Ag doping. *Chem. Commun.* **2010**, *46*, 4713–4715.
- (37) Joshi, C. P.; Bootharaju, M. S.; Alhilaly, M. J.; Bakr, O. M. [Ag₂₅(SR)₁₈][−]: The “Golden” silver nanoparticle. *J. Am. Chem. Soc.* **2015**, *137*, 11578–11581.
- (38) Krishnadas, K. R.; Baksi, A.; Ghosh, A.; Natarajan, G.; Pradeep, T. Structure-conserving spontaneous transformations between nanoparticles. *Nat. Commun.* **2016**, *7*, 13447.
- (39) Zhang, B.; Salassa, G.; Bürgi, T. Silver migration between Au₃₈(SC₂H₄Ph)₂₄ and doped Ag_xAu_{38-x}(SC₂H₄Ph)₂₄ nanoclusters. *Chem. Commun.* **2016**, *52*, 9205–9207.
- (40) Knoppe, S.; Dolamic, I.; Bürgi, T. Racemization of a Chiral Nanoparticle Evidences the Flexibility of the Gold–Thiolate Interface. *J. Am. Chem. Soc.* **2012**, *134*, 13114–13120.
- (41) Salorinne, K.; Malola, S.; Wong, O. A.; Rithner, C. D.; Chen, X.; Ackerson, C. J.; Häkkinen, H. Conformation and dynamics of the ligand shell of a water-soluble Au₁₀₂ nanoparticle. *Nat. Commun.* **2016**, *7*, 10401.
- (42) AbdulHalim, L. G.; Bootharaju, M. S.; Tang, Q.; Del Gobbo, S.; AbdulHalim, R. G.; Eddaoudi, M.; Jiang, D.-e.; Bakr, O. M. Ag₂₉(BDT)₁₂(TPP)₄: A tetravalent nanocluster. *J. Am. Chem. Soc.* **2015**, *137*, 11970–11975.
- (43) Ghosh, A.; Ghosh, D.; Khatun, E.; Chakraborty, P.; Pradeep, T. Unusual reactivity of dithiol protected clusters in comparison to monothiol protected clusters: studies using Ag₅₁(BDT)₁₉(TPP)₃₀ and Ag₂₉(BDT)₁₂(TPP)₄. *Nanoscale* **2017**, *9*, 1068–1077.
- (44) Yamazoe, S.; Takano, S.; Kurashige, W.; Yokoyama, T.; Nitta, K.; Negishi, Y.; Tsukuda, T. Hierarchy of bond stiffnesses within icosahedral-based gold clusters protected by thiolates. *Nat. Commun.* **2016**, *7*, 10414.
- (45) Tlahuice-Flores, A.; Black, D. M.; Bach, S. B. H.; Jose-Yacamán, M.; Whetten, R. L. Structure & bonding of the gold-subhalide cluster I-Au₁₄₄Cl₆₀^[2]. *Phys. Chem. Chem. Phys.* **2013**, *15*, 19191–19195.
- (46) Xu, W. W.; Zhu, B.; Zeng, X. C.; Gao, Y. A grand unified model for liganded gold clusters. *Nat. Commun.* **2016**, *7*, 13574.
- (47) Natarajan, G.; Mathew, A.; Negishi, Y.; Whetten, R. L.; Pradeep, T. A unified framework for understanding the structure and modifications of atomically precise monolayer protected gold clusters. *J. Phys. Chem. C* **2015**, *119*, 27768–27785.
- (48) Heinecke, C. L.; Ni, T. W.; Malola, S.; Mäkinen, V.; Wong, O. A.; Häkkinen, H.; Ackerson, C. J. Structural and theoretical basis for ligand exchange on thiolate monolayer protected gold nanoclusters. *J. Am. Chem. Soc.* **2012**, *134*, 13316–13322.
- (49) Bootharaju, M. S.; Joshi, C. P.; Parida, M. R.; Mohammed, O. F.; Bakr, O. M. Templated atom-precise galvanic synthesis and structure elucidation of a [Ag₂₄Au(SR)₁₈][−] nanocluster. *Angew. Chem.* **2016**, *128*, 934–938.
- (50) Bhat, S.; Baksi, A.; Mudedla, S.; Natarajan, G.; Subramanian, V.; Pradeep, T. Au₂₂Ir₃(PET)₁₈: An unusual alloy cluster through inter-cluster reaction. *J. Phys. Chem. Lett.* **2017**, *8*, 2787–2793.
- (51) Yoon, B.; Luedtke, W. D.; Gao, J.; Landman, U. Diffusion of Gold Clusters on Defective Graphite Surfaces. *J. Phys. Chem. B* **2003**, *107*, 5882–5891.
- (52) Ghosh, A.; Pradeep, T.; Chakraborty, J. Coalescence of atomically precise clusters on graphenic surfaces. *J. Phys. Chem. C* **2014**, *118*, 13959–13964.
- (53) Som, A.; Samal, A. K.; Udayabhaskararao, T.; Bootharaju, M. S.; Pradeep, T. Manifestation of the difference in reactivity of silver clusters in contrast to its ions and nanoparticles: the growth of metal tipped Te nanowires. *Chem. Mater.* **2014**, *26*, 3049–3056.
- (54) Xia, N.; Wu, Z. Doping Au₂₅ nanoparticles using ultrasmall silver or copper nanoparticles as the metal source. *J. Mater. Chem. C* **2016**, *4*, 4125–4128.
- (55) Kabbani, M. A.; Tiwary, C. S.; Autreto, P. A. S.; Brunetto, G.; Som, A.; Krishnadas, K. R.; Ozden, S.; Hackenberg, K. P.; Gong, Y.; Galvao, D. S.; Vajtai, R.; Kabbani, A. T.; Pradeep, T.; Ajayan, P. M. Ambient solid-state mechano-chemical reactions between functionalized carbon nanotubes. *Nat. Commun.* **2015**, *6*, 7291.
- (56) Kabbani, M. A.; Tiwary, C. S.; Som, A.; Krishnadas, K. R.; Autreto, P. A. S.; Ozden, S.; Keyshar, K.; Hackenberg, K. P.; Chipara, A. C.; Galvao, D. S.; Vajtai, R.; Kabbani, A. T.; Pradeep, T.; Ajayan, P. M. A generic approach for mechano-chemical reactions between carbon nanotubes of different functionalities. *Carbon* **2016**, *104*, 196–202.